An Ellipsometric Study of Polymer Monolayers at the Air/Water Interface

Bryan B. Sauer,† Hyuk Yu,† Mehran Yazdanian,‡ and George Zografi‡

Department of Chemistry and School of Pharmacy, University of Wisconsin, Madison, Wisconsin 53706

Mahn Won Kim*

Exxon Research and Engineering Company, Annandale, New Jersey 08801.
Received July 18, 1988; Revised Manuscript Received October 31, 1988

ABSTRACT: Monolayers of poly(ethylene oxide) (PEO), (hydroxypropyl)cellulose (HPC), poly(vinyl acetate) (PVAc), and poly(methyl methacrylate) (PMMA) were studied at the air/water interface. The change in ellipsometric phase angle, $\delta\Delta$, was measured with a recently constructed, sensitive-phase-modulated instrument as a function of surface concentration, Γ. At the same time, the static surface pressure, Π, was monitored. The $\delta\Delta$ values for PEO and HPC rise rather monotonically with increasing Γ and then reach a plateau as the monolayers collapse, paralleling the plateau in the Π–A isotherm. The plateau is attributed to the solubilization of chain segments in the aqueous phase. Both PEO and HPC are water soluble, but $\delta\Delta$ is much larger in magnitude for HPC, which we interpret in terms of steric effects of the HPC chain structure. PVAc, which is water insoluble, also shows a monotonic increase in $\delta\Delta$ with Γ, but unlike PEO, $\delta\Delta$ continues to increase, which is interpreted as the chain pileup on the surface due to macroscopic collapse. The more condensed monolayer of PMMA shows a large increase in $\delta\Delta$, even in the surface concentration region where $\Pi = 0$, which can be explained by the presence of condensed islands of polymer on the surface. In the higher concentration region where Π increases from 0 to 26 dyn/cm, the values of $\delta\Delta$ also increase steadily. Analyses of the ellipsometric data, assuming constant film thickness, indicate that the increase in $\delta\Delta$ over a wide range of Γ can be ascribed to an increase in mass density, hence to an increase in the film refractive index. By use of this model, film thicknesses of 3.4 ± 0.2, 8.0 ± 0.5, 6.0 ± 0.5, and 14.0 ± 0.5 Å were deduced for PEO, HPC, PVAc, and PMMA, respectively.

Introduction

Ellipsometry has been shown to be quite useful in the study of partially covered air/liquid interfaces where the liquid subphase consists of a high refractive index material such as mercury.[1] The reduced contrast in refractive index at the air/water interface has limited the types of monolayer systems studied by conventional null detection ellipsometric methods and in some cases has introduced uncertainties. Such experimental uncertainties have been responsible for the death of experiments reported at the air/water interface;[2-9] we have recently attempted to correct the situation with use of a phase-modulated instrument with improved sensitivity.[10] The work presented here is related to those reported recently by Kawaguchi et al.[8,9] in which some of the same polymer monolayer systems are studied. Although our raw experimental results in terms of the ellipsometric phase angle, $\delta\Delta$, are qualitatively similar, there are several discrepancies because of the different analysis schemes used. In light of these discrepancies, we will make detailed comparisons with their results later in this paper.

The objective of this paper is to elucidate some of the fundamental aspects of ellipsometry applied to partially to fully covered liquid surfaces for several horizontally oriented polymer monolayers of varying hydrophilicity. The calibration of the phase-modulated ellipsometry instrument used in this study has been reported elsewhere[11] using a series of fatty acids with different chain lengths at the air/water interface. Controlling the fractional coverage, θ, on a liquid surface by a spreading technique allowed us to pursue the questions raised in previous ellipsometric experiments[12-14] with small molecules adsorbed on solid substrates, where the surface mass density could not be explicitly defined or controlled. If the experiments are performed as a function of surface density and the results are compared with various ellipsometric predictions, polymer interfacial conformation and surface structure can be deduced, thus leading to a general picture for polymer adsorption, independent of the hydrophilicity of the polymer.

Polymers which form monolayers of the expanded and condensed types[15,16] were chosen because of the controllability of surface mass density and of its importance in ellipsometry. For polymers, the two-dimensional segment density on the air/water interface is largely controlled by the polymer hydrophilicity. PEO and PVAc[15] are classified as expanded type monolayers with low segment–segment cohesion at the interface leading to a relatively low segment density at a given surface pressure. Their surface pressure–surface concentration (Π–Γ) isotherms are in good agreement with the scaling predictions for chain configuration in two dimensions under "good surface solvent conditions" at A/W.[17-20] Ries and Walker[21] reported in 1961 that PVAc monolayers by themselves were not detected by electron microscopy because of their horizontal orientation. They thus resorted to mixing PVAc with vertically oriented surfactants to monitor the collapse of PVAc in these mixtures when transferred onto solid substrates.

PMMA forms a condensed monolayer[16] with the chains in a relatively close-packed conformation at the A/W interface due to the strong segment–segment cohesion. The Π–Γ isotherm has been shown to scale closely according to the scaling predictions for polymers in the two-dimensional "surface theta state" at A/W.[17] The thickness of PMMA monolayers transferred to solid substrates determined ellipsometrically by Gabrielli and Guarini[22] are in qualitative agreement with our in situ results. HPC is water soluble and forms a condensed monolayer due to the strong segment–segment interaction between the bulky chain segments. It provides an interesting comparison with PEO which is also water soluble.

Theoretical Background

The amplitude reflection coefficients (R_p and R_s) describing the polarization characteristics of the incident and

† Department of Chemistry.
‡ School of Pharmacy.

0024-9297/89/2222-2332$01.50/0

reflected beams are related to the two ellipsometric angles, the amplitude attenuation (ψ), and phase difference (Δ) between the orthogonal p and s waves:[23]

$$R_p/R_s = \tan \psi \exp(i\Delta) \quad (1)$$

Equation 2 gives the reflection coefficients (R_p and R_s) for the case where different subscripts stand for three distinct layers, namely, layer 0 is air, layer 1 the film, and layer 2 the aqueous phase:

$$R = [r_{01} + r_{12} \exp(-i\beta)]/[1 + r_{01}r_{12} \exp(-i\beta)] \quad (2)$$

where

$$\beta = 4\pi n_1 d_1 \cos \phi_1/\lambda \quad (3)$$

and n_1 is the average refractive index of the film, d_1 is the film thickness, ϕ_1 is the incident angle in the film, and λ is the laser wavelength (6328 Å). Equation 2 is valid either for p or s polarization, and

$$r_{p01} = [n_1 \cos \phi_0 - n_0 \cos \phi_1]/[n_1 \cos \phi_0 + n_0 \cos \phi_1] \quad (4)$$

$$r_{s01} = [n_0 \cos \phi_0 - n_1 \cos \phi_1]/[n_0 \cos \phi_0 + n_1 \cos \phi_1] \quad (5)$$

where r_{p01} and r_{s01} are the Fresnel coefficients for the reflection between layer 0 and layer 1. Similar expressions for r_{p12} and r_{s12} are used for layer 1 and layer 2 to allow the calculation of Δ via eq 1. The incident angles for layers 1 and 2 are calculated by using Snell's law along with an incident angle in air of 64.1° and the refractive indices n_0 = 1.002 for air, n_2 = 1.332 for water, and an estimated average refractive index n_1 for the film which depends on the polymer and fractional coverage, θ.

The experiments are performed by first determining Δ for the clean water surface and then at various polymer surface densities, Δ', with the change in phase angle, $\delta\Delta$, between these two states defined as

$$\delta\Delta = \Delta' - \Delta \quad (6)$$

To give positive values of $\delta\Delta$ at the air/water interface, eq 6 is defined here in the reverse of the usual convention.[14] By solving eq 1 numerically, it is found that the thickness, d_1, and the ellipsometric phase angle, $\delta\Delta$, are directly proportional:

$$\delta\Delta = \alpha d_1 \quad (7)$$

Various approximate formulas are available for conveniently determining the proportionality constant, α; note that there are typographical errors in eq 2 of ref 13 and eq 13 of ref 14. Even though the full Drude equations (eq 1) were used for all comparisons with experiments, the approximate equations were found to be quite accurate as long as the film thickness is much less than the wavelength of light. For example, by use of d_1 = 10 Å and n_1 = 1.00–2.00, the approximate expression for α at air/water gave thicknesses within 0.02% of those calculated by the full equation, and for d_1 = 100 Å it was within 5%. One other important result of both the approximate and full Drude equations is that $\delta\psi$ ($\delta\psi = \psi - \psi'$) is essentially zero[6] for thin films if the substrate is nonadsorbing. This indicates that, for nonadsorbing films, monolayer information can only be obtained from the value of $\delta\Delta$ at the air/water interface, and no $\delta\psi$ values were measured in this report.

Models of Inhomogeneous Monolayers. Normally the dielectric material in the film is characterized by the macroscopic parameters, index of refraction (n_1) and thickness (d_1). To compare predicted values of $\delta\Delta$ with the experimentally measured values, a model for the monolayer has to be assumed. If one considers the full range of θ, from barely occupied, $\theta \ll 1$, to the case of fully occupied, $\theta \approx 1$, then several models can be envisioned including the ones presented in Figure 1.

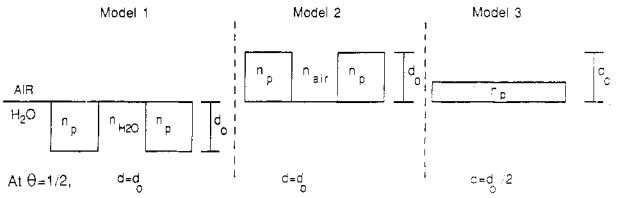

Figure 1. Monolayer models.

Model 1 describes the microscopic features of the inhomogeneous film by using an effective macroscopic refractive index (n_1, Figure 1) which is an average of the polymer (n_p) and water (n_2) refractive indices. Model 2 is similar to model 1 except that the refractive index of air (n_0) is averaged with the polymer refractive index. It seems reasonable that the thickness would not change significantly as the monolayer was compressed if no drastic conformation change took place. Thus, we assume the thickness remains constant as n_1 varies at different film densities for both of these models. To calculate the refractive index for films where the coverage normally varies for $0.05 \leq \theta \leq 1$ requires additional assumptions as to the dependence of n_1 on θ. To estimate n_1, the Lorentz–Lorenz equation[24] is used for ideal mixtures:

$$(n_1^2 - 1)/(n_1^2 + 2) = \theta(n_p^2 - 1)/(n_p^2 + 2) + (1 - \theta)(n^2 - 1)/(n^2 + 2) \quad (8)$$

where $n = n_2$ for model 1 and $n = n_0$ for model 2. Thus, the film refractive index is described as that of a water-swollen polymer, with the polymer content determined by θ for model 1 (or for model 2, polymer "swollen with air"). Because of the small refractive index difference between polymer and substrate, n_1 calculated by taking an arithmetic mean of n_p^2 and n_2^2 of polymer and water, respectively, gives essentially the same results as those deduced by eq 8. In practice, eq 8 is solved for an average film refractive index (n_1) at various values of θ (corresponding to the surface concentration, Γ). The values of n_1 are then substituted into eq 1 to calculate predicted values of $\delta\Delta$.

Model 3 (in Figure 1) considers a continuous film with $n_1 = n_p$ = constant, where n_p is the refractive index of the bulk polymer. In this model, the thickness, d, increases linearly with the fractional coverage, θ, as in $d = \theta d_0$ where d_0 is the thickness of the full monolayer. There are conceptual difficulties in using model 3 for partially covered surfaces because at $\theta \ll 1$ the calculated thickness becomes fractional atomic dimension. For example, if the bulk refractive index of n_1 = 1.455 for PEO[25] is inserted in eq 1, a value of α = 0.0353 deg/Å is calculated, where α is the proportionality constant in eq 7. For $\delta\Delta$ = 0.01°, which is a typical value for PEO at low coverage, $d \approx$ 0.28 Å, which is not reasonable. Thus, model 3 will not be considered further in attempts to compare with the experimental results even though it does predict the same linear dependence as the microscopic models.

Microscopic models[10,13,14,26] consider that the partially covered surface contains a distribution of scattering centers in two dimensions. The analogue of eq 7 predicted by this theory is[13]

$$\delta\Delta = \sum \alpha_i' \sigma_i \quad (9)$$

where $i(x,y,z)$ and α_i' is a proportionality constant. Since σ_i is the concentration of scattering centers per unit area,

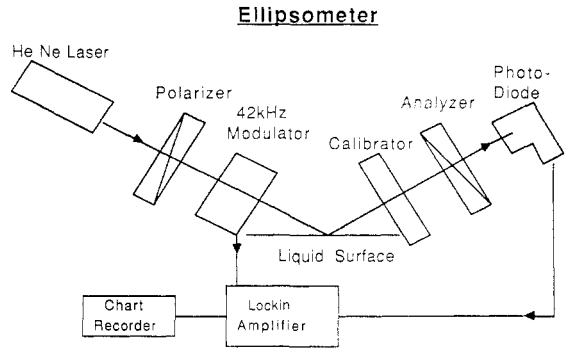

Figure 2. Block diagram of the ellipsometry instrument.

a reasonable assumption is that $\sigma_i = \theta\sigma_i'$. Thus, the predicted $\delta\Delta$ should be directly proportional to θ. Hall[27] has argued on theoretical grounds that $\sigma_i = \theta^{1/2}\sigma_i'$ should be the case. However, the $\theta^{1/2}$ dependence has never been seen experimentally.[1,8,28] The one limitation of these microscopic models relative to providing any insight into the molecular conformation at the interface lies in the fact that they address nothing about macroscopic parameters such as the thickness or refractive index.

Experimental Section

Materials. PEO was purchased from Toyo Soda Company (supplied by Varian Associates, Sunnyvale, CA) and a 252K fraction was used with $M_w/M_n = 1.04$; here K stands for kilodalton in molecular weight units. The characterized HPC sample (Hercules, lot 3464) was a gift of Eugene McNally. It was found to have a viscosity-average molecular weight of 843K and a polydispersity measure of $M_w/M_n < 2.2$ as determined by GPC. PVAc was polymerized as reported previously, and the molecular weights of different fractions were determined by intrinsic viscosity.[19] A fraction with M_w of 114K was used. The molecular weight of a fractionated PMMA sample was also determined by intrinsic viscosity in benzene, and a 98K sample was used. The polydispersities of the PVAc and PMMA fractions were not determined, but the static surface pressures have been found to be independent of molecular weight over a wide range,[15,17,19] indicating that polydispersity would not affect the results.

A 1:1 mixture of chloroform (Fisher Scientific, ACS grade) and methanol (Aldrich, HPLC grade) was used as the spreading solvent for HPC, and dichloromethane (Fisher, ACS grade) was used as a spreading solvent for the other three polymers. The concentrations of the spreading solutions were between 1 and 2 mg/mL.

The water used as distilled water further purified with a Milli-Q filtering system (Millipore) with one carbon and two ion-exchange filters.

Methods. All experiments were performed at room temperature (23.0 ± 0.2 °C) on a Lauda balance; surface pressue was measured by the standard Langmuir film balance technique, which measures the actual surface force between a clean surface and a monolayer covered surface using a strain gauge. The overall sensitivity was ±0.05 dyn/cm. The Teflon-coated trough had a maximum area of 700 cm^2. The polymer surface concentrations were controlled by the addition method or with a sliding Teflon barrier. The surface was cleaned by aspiration and checked before each run by compressing 30-fold to produce a surface pressure change of less than 0.1 dyn/cm. At least 30 min were allowed for water vapor pressure equilibration, which contributed to base-line drift in the ellipsometric experiments.

A block diagram of the instrument is shown in Figure 2. Our design was based on the principle of modulation ellipsometry.[23] The majority of the experiments were performed on a optical table. Floating the table on an air cushion increased the signal-to-noise ratio by a factor of 10 but introduced some base-line drift due to a slow shifting of the table. The experiments were performed at a fixed incident angle (64.1 ± 0.1°) measured relative to the axis normal to the surface by using an unfocused 5-mW He–Ne laser with a beam width of about 1 mm. The important component which gives high sensitivity at the air/water interface is the photoelastic modulator (Hinds International, Portland, OR, PEM-80) which introduces a periodic relative phase shift between orthogonal amplitude components at a frequency of 42 kHz. Reflection from the surface causes additional phase shift and amplitude attenuation, and the phase shift was detected in the analog mode by locking into the modulation frequency.

The calibrator was used to perform a manual calibration of the instrument before and after a monolayer experiment, but the calibrator had no function during the actual determination of $\delta\Delta$ from a monolayer-covered surface. An increment in the calibrator corresponded to a known change in Δ, giving a relationship between the voltage measured on the chart recorder and Δ in degrees.

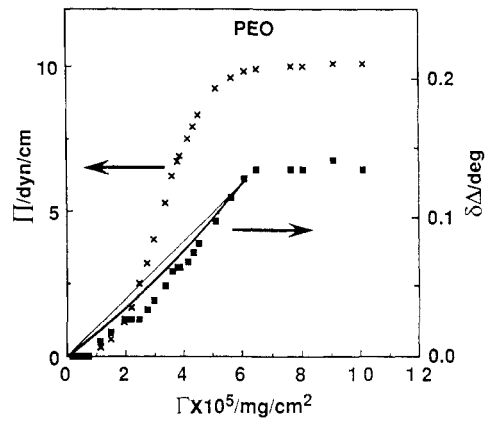

Figure 3. Surface pressure (Π) and the change in ellipsometric phase angle ($\delta\Delta$) versus surface concentration (Γ) for 252K PEO. The thick solid curve (model 1 from Figure 1) and thin line (microscopic model) are predictions (see text). The plateau in $\delta\Delta$ at high Γ is ascribed to the solubilization of PEO segments into the aqueous subphase.

Results

All the monolayer results are presented in terms of the change in ellipsometric phase angle, $\delta\Delta$, and surface pressure, Π, versus the surface concentration, Γ. The values of $\delta\Delta$ predicted by the various models are represented as continuous curves in the various figures. Further comments on these predicted values will be deferred to the Discussion section. In Figure 3 the results for 252K PEO show that $\delta\Delta$ remains at 0 until $\Gamma = 0.8 \times 10^{-5}$ mg/cm^2. It then rises monotonically as the surface pressure increases. As Π reaches its collapse pressure of 10 dyn/cm at $\Gamma = 6 \times 10^{-5}$ mg/cm^2, $\delta\Delta$ also reaches a plateau of 0.13°. Since PEO is water soluble, we attribute this to collapse of segments into the aqueous phase. The lack of contrast between the refractive index of water and the collapsed segments would explain the absence of any additional change in $\delta\Delta$. This is quite different from water-insoluble PVAc as will be seen presently.

HPC is a water-soluble polymer which is also quite surface active because of its amphiphilic nature. Since it forms a more condensed monolayer than PVAc, we present the results here to make direct comparison with the other water soluble polymer, PEO. In Figure 4 for 843K HPC, it is evident that $\delta\Delta$ increases monotonically with surface density in the region $\Gamma = (0\text{–}3) \times 10^{-5}$ mg/cm^2 irrespective of Π, which remains constant at $\Pi = 0$ in this low concentration region. This indicates that $\delta\Delta$ is mainly dependent on θ. There is a little scatter in $\delta\Delta$ because different compression runs were spliced together an the precision of the experiment is about 0.005° (corresponding to approximately 0.1-Å thickness). Even when Π starts to increase at $\Gamma = 3 \times 10^{-5}$ mg/cm^2, $\delta\Delta$ continues to increase monotonically until the monolayer collapses at $\Gamma = 15 \times 10^{-5}$ mg/cm^2. As in the case of PEO, we explain the plateau in terms of the water-soluble HPC segments desorbing into the aqueous phase. The magnitude of $\delta\Delta$ at the plateau is more than 5 times greater than that for

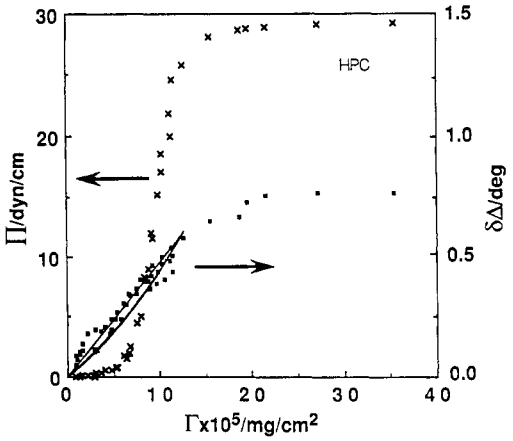

Figure 4. Surface pressure (Π) and the change in ellipsometric phase angle (δΔ) versus surface concentration Γ for 843K HPC. The thin line and thick solid curve have the same significance as in Figure 3. The plateau in δΔ at high Γ is also ascribed to the solubilization of HPC segments into the aqueous subphase.

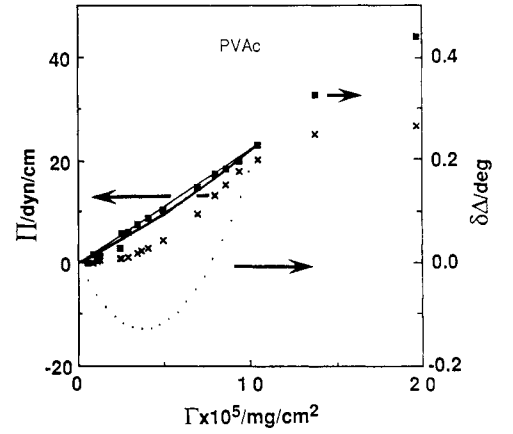

Figure 5. Surface pressure (Π) and the change in ellipsometric phase angle (δΔ) versus surface concentration Γ for 114K PVAc in the lower concentration region. The thin line (microscopic model), thick solid curve (model 1), and dotted curve (model 2) are predictions (see text).

PEO because of a difference in refractive index and thickness of the two polymers.

The results for 114K PVAc are given in Figure 5 along with theoretical predictions (solid and dotted curves) which will be discussed in the next section. The values of δΔ are 0 until $\Gamma = 0.8 \times 10^{-5}$ mg/cm², and they begin to increase while the surface pressure is 0 until about $\Gamma = 1.5 \times 10^{-5}$ mg/cm². This indicates once again that δΔ is sensitively dependent on the fraction coverage, θ, irrespective of Π. The surface pressure increases slowly at low concentrations, while δΔ increases rather monotonically even after Π begins to increase more rapidly at $\Gamma = 5 \times 10^{-5}$ mg/cm². At $\Gamma = 13 \times 10^{-5}$ mg/cm², Π reaches a plateau, yet δΔ still increases at about the same rate. the Π–Γ isotherm is reversible to a certain extent up to 20 dyn/cm, although there is some hysteresis upon expansion after annealing for more than 10 min at Π above 15 dyn/cm. There was never any detectable hysteresis in δΔ, so we conclude that no desorption occurs for the 114K PVAc sample.

Results are shown for 114K PVAc in Figure 6 over a concentration range well past collapse to make contact with a report in the literature.[21] It is evident from these results that, as the PVAc monolayer collapses between $\Gamma = 12 \times 10^{-5}$ and 30×10^{-5} mg/cm², there is an inflection in δΔ. This appears because at this point, not only is the density increasing, but the monolayer is thickening in the form of a multilayer. Multilayer formation was visualized by ex-

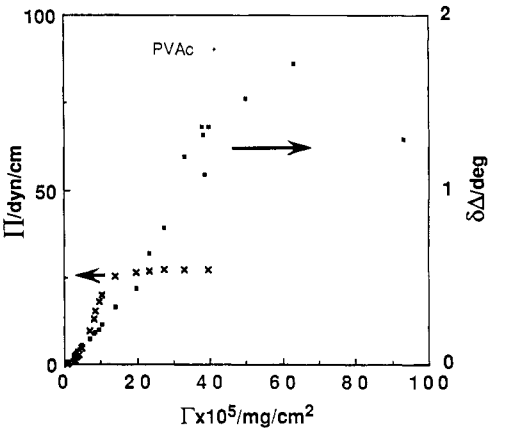

Figure 6. Surface pressure (Π) and the change in ellipsometric phase angle (δΔ) versus surface concentration Γ for 114K PVAc. Several points at higher Γ are presented along with the data in Figure 5. A dramatic change in δΔ is seen starting at Γ of about 38×10^{-5} mg/cm² as macroscopic collapse takes place. The scatter in this region is due to inhomogeneities in the monolayer.

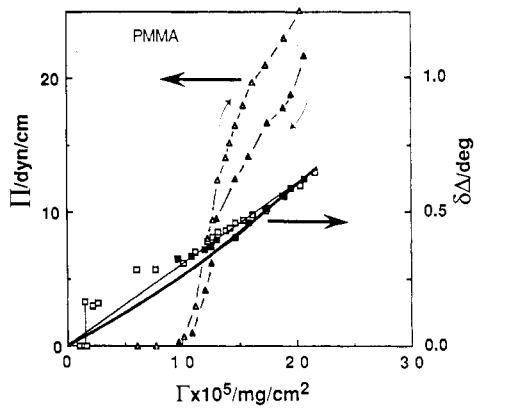

Figure 7. Surface pressure (Π) and the change in ellipsometric phase angle (δΔ) versus surface concentration (Γ) for 98K PMMA for full compression and expansion cycles. Hysteresis was present in the surface pressure for the compression–expansion cycle where open triangles are for the compression branch and filled triangles are for the expansion branch, but within experimental error there was no hysteresis in δΔ (open and filled squares represent compression and expansion, respectively). The thin line (microscopic model) and thick solid curve (model 1) are predictions. At low Γ, the values of δΔ fluctuate between 0 and 0.18°, which can be attributed to inhomogeneities in the monolayer.

amining the small-angle scattering of the beam reflected from the monolayer. Large inhomogeneities in the film could be seen from the small-angle scattering at concentrations above 38×10^{-5} mg/cm², consistent with the microscopic observations of Ries and Walker for mixed films of PVAc and stearic acid at surface pressures above the collapse pressure.[21] This sample has a very similar Π–Γ isotherm to PEO, yet the ellipsometric results are remarkably different in the collapse region, indicating that ellipsometry is a useful tool in the highly packed, surface pressure independent regions.

The 98K PMMA sample shows a large hysteresis in Π, so one full cycle of compression and expansion was performed. For each point in Figure 7 the surface pressure was allowed to equilibrate for at least 10 min. This sample forms a condensed monolayer and is known to be inhomogeneous at low monolayer coverage.[15] Evidence for these inhomogeneities, which we refer to as patches, is given in Figure 7 where the ellipsometric values for δΔ vary between 0 and 0.18° at concentrations between $\Gamma = 1 \times 10^{-5}$ and 2×10^{-5} mg/cm². The value of δΔ is 0 if no condensed material is illuminated by the beam and increases to around 0.18° when patches are partly or com-

Table I
Macroscopic Constants for Polymer Monolayers at 23 °C

	at $\theta = 1$					
	$\delta\Delta$, deg	$10^5\Gamma$, mg/cm^2	n	d_1,[c] Å	d_{calc},[d] Å	ρ, g/cm^3
PEO	0.13	6.0	1.455[a]	3.4 ± 0.2	5.5	1.1[e]
HPC	0.64	12.5	1.559[b]	8.0 ± 0.5	11.4	1.1[b]
PVAc	0.23	10.0	1.465[a]	6.0 ± 0.5	8.4	1.19[a]
PMMA	0.67	23.0	1.490[a]	14.0 ± 0.5	19.4	1.19[a]

[a] Reference 25. [b] Reference 29 [c] See text for the discussion of assumptions used in determining d_1. [d] These values are estimated from the ratios of Γ (in the second column) and the bulk polymer density, ρ (in the last column). [e] Reference 30.

pletely illuminated. The values of $\delta\Delta$ increase slowly from around 0.2° to 0.4° between $\Gamma = 2$ and 8×10^{-5} mg/cm^2 even though $\Pi = 0$ in this dilute region and continue to rise monotonically as Π increases, starting at $\Gamma = 10 \times 10^{-5}$ mg/cm^2 which is the point where Π begins to increase sharply.

As mentioned before, the Π–Γ isotherm for PMMA exhibits quite a large hysteresis upon compression or expansion even when at least 20-min equilibration periods were allowed for each point. When compressing, Π *overshoots* and then slowly decreases and eventually stops decreasing after several minutes. When expanding, Π *undershoots* and then slowly increases. The values of $\delta\Delta$ do not show any hysteresis within experimental error and show absolutely no time dependence, even though the surface pressure can vary by 100% upon compression. It is tempting to speculate that the hysteresis in Π is due to segment rotation as the acrylate groups reorient toward the interface, while the thickness remains unaffected by this change.

Discussion

Clearly all of the ellipsometric data generated increase rather monotonically with θ. This would be expected if $\delta\Delta$ depends mainly on the film density, which in turn controls the film refractive index, n_1. To make use of models 1 and 2, some assumptions concerning n_1 must be made. For all the polymers, we have chosen the surface concentration at the onset of the plateau in Π to represent $\theta = 1$, the fully covered state, and we have assumed that $n_1 = n_p$ at this point. These values of Γ and n_p are given in Table I. Next, the experimental value of $\delta\Delta$ at $\theta = 1$ is used to calculate the thickness, d_1, using the Drude equations (eq 1) and setting $n_1 = n_p$. The thicknesses thus determined, given in Table I, vary from 3.4 Å for PEO to 14 Å for PMMA. Keeping d_1 constant, the average film refractive index, n_1, was then back-calculated by using eq 8 for $0 \leq \theta \leq 1$. Inserting these values of n_1 into eq 1 gives the thick solid curves in Figures 3–5 and 7.

We should now make a comparison with the recent results of Kawaguchi et al.[8,9] who have extracted both d_1 and n_1 using the Drude equations. Since they state that $\delta\psi$ was zero for PEO and PMMA over the entire concentration region, it is not obvious how they obtained reliable values for both d_1 and n_1. We find their claim of segments dangling into the water on the order of 100's Å inconsistent with our results in Table I, especially for the water-insoluble materials. On the other hand, their $\delta\Delta$ values are quite similar, and the discussion of $\delta\Delta$ as a function of θ in this report is equally applicable to their results.

The self-consistency of our calculated thicknesses at $\theta = 1$ can be checked by dividing the values of Γ listed in the second column of Table I by the bulk polymer density, giving units of thickness. These predicted values of d_1 agree quite well with those determined using the experimental values of $\delta\Delta$ for all the polymers. The fact that the predicted values are consistently 30% higher could be due to the obscuring of the sharpness of the interface or film by vibrations, segment desorption, or a number of other factors as yet unknown contributing to a nonuniform concentration profile normal to the interface. Another explanation is the possibility of refractive index anisotropy due to chain orientation parallel with the interface. By use of the Drude equations for anisotropic thin films,[6] a small anisotropy for the PMMA monolayer such as $n_z = 1.51$ and $n_x = n_y = 1.47$, where n_z is the refractive index normal to the surface, would explain the 30% difference. Similar magnitudes of the refractive index anisotropy would also increase the thicknesses by approximately 30% for the other three polymers. Unfortunately, detailed knowledge of the polymer conformation would be needed to estimate the anisotropy by summing individual bond polarizabilities.

Returning to the θ dependence, the trend in the experimental $\delta\Delta$ values for PEO in Figure 3 is similar to that predicted by model 1 (thick solid curve). The agreement with linear dependence (thin solid line in Figure 3) of $\delta\Delta$ on θ which would be predicted by microscopic theories also seems to qualitatively fit the data, and because of the low ellipsometric contrast of PEO, it cannot be determined which model fits experiment better.

Within experimental error, both the linear dependence (thin line) and that predicted by model 1 (thick solid curve) follow the trends in the data for HPC in Figure 4.

For PVAc in Figure 5, the predictions of three different models are included. Once again, both the linear dependence (thin line) and model 1 (thick curve) fit the data well. On the other hand, using model 2 by averaging the refractive index of air with the polymer refractive index when calculating n_1 initially gives negative values of $\delta\Delta$ before reaching the same value as model 1, where θ is set to unity at $\Gamma = 10 \times 10^{-5}$ mg/cm^2. The negative values are expected for model 2 when the film refractive index is less than 1.332 (see the calculations in Appendix of ref 1). Since the experimental results do not become negative, we have a strong case for model 1 as far as the macroscopic models are concerned. The predictions of model 2 have a similar trend for all other polymers; hence they are not graphed.

PMMA is unique among these samples because it forms an inhomogeneous monolayer at low concentrations. Since the islands of condensed material are similar in size to the laser beam, no theories are expected to hold in the dilute region. This is evident in Figure 7 where both the thin line and thick curve are below the experimental $\delta\Delta$. In the higher concentration region, the best fit with theory cannot be discerned within experimental error; both microscopic and macroscopic predictions seem to agree with experiment.

Summary

A series of four polymers of varying hydrophilicity spread as monolayers at the A/W interface were studied ellipsometrically over a wide range of fractional coverage, θ. It was shown that ellipsometry is a sensitive tool in the study of partial film to full film coverage, as well as for films in the collapsed state. Thicknesses have been determined which are physically reasonable based on packing efficiency and monomer size. The thickness was found to increase in the order PEO, PVAc, HPC, and PMMA with all values less than 15 Å.

The dependence of the experimentally measured $\delta\Delta$ on fractional coverage, θ, has been modeled using the Drude equations assuming constant thickness. To fit the data,

the film refractive index was calculated by using the Lorentz–Lorenz equation which assumes an average of water and polymer refractive indices. Hence, our picture of the polymer monolayer is that of an extremely hydrated one. Microscopic models which take into account individual molecular polarizability[10,13,14,26] predict that $\delta\Delta$ is linear with θ. Unfortunately, within experimental error we cannot discern between linear dependence and that obtained by calculating the average refractive index with the Lorentz–Lorenz equation for the polymers studied here. Further experiments with other monolayers of higher ellipsometric contrast are in progress to address this issue.

Acknowledgment. This work is in part supported by the Research Committee of the University of Wisconsin—Madison and the Procter and Gamble Company.

Registry No. PEO, 25322-68-3; HPC, 9004-64-2; PVAc, 9003-20-7; PMMA, 9011-14-7.

References and Notes

(1) Smith, T. *J. Opt. Soc. Am.* **1968**, *58*, 1069.
(2) de Feijter, J. A.; Benjamins, J.; Veer, F. A. *Biopolymers* **1978**, *17*, 1759.
(3) Graham, D. E.; Phillips, M. C. *J. Colloid Interface Sci.* **1979**, *70*, 415.
(4) Kawaguchi, M.; Oohira, M.; Tajima, M.; Takahashi, A. *Polym. J. (Tokyo)* **1980**, *12*, 849.
(5) de Feijter, J. A.; Benjamins, J. *J. colloid Interface Sci.* **1981**, *81*, 91.
(6) den Engelsen, D.; de Koning, B. *J. Chem. Soc., Faraday Trans. 1* **1974**, *70*, 1603.
(7) den Engelsen, D.; de Koning, B. *J. Chem. Soc., Faraday Trans. 1* **1974**, *70*, 2100.
(8) Kawaguchi, M.; Yohyama, M.; Mutoh, Y.; Takahashi, A. *Langmuir* **1988**, *4*, 407.
(9) Kawaguchi, M.; Yohyama, M.; Takahashi, A. *Langmuir* **1988**, *4*, 411.
(10) Rasing, Th.; Hsiung, H.; Shen, Y. R.; Kim, M. W. *Phys. Rev. A* **1988**, *37*, 2732.
(11) Kim, M. W.; Sauer, B. B.; Yu, H.; Yazdanian, M.; Zografi, G., to be submitted for publication.
(12) Archer, R. *J. Opt. Soc. Am.* **1962**, *52*, 970.
(13) Archer, R. J. In *Ellipsometry in the Measurement of Surfaces and Thin films*; Passaglia, E., Stromberg, R. R., Kruger, J., Eds.; NBS Miscellaneous Publication 256; U.S. Government Printing Office: Washington, DC, 1964; p 255.
(14) Bootsma, G. A.; Meyer, F. *Surf. Sci.* **1969**, *14*, 52.
(15) Crisp, D. J. *J. Colloid Sci.* **1946**, *1*, 49.
(16) Crisp, D. J. *J. Colloid Sci.* **1946**, *1*, 161.
(17) Vilanove, R.; Rondelez, F. *Phys. Rev. Lett.* **1980**, *45*, 1502.
(18) Kawaguchi, M.; Komatsu, S.; Matsuzumi, M.; Takahashi, A. *J. Colloid Interface Sci.* **1984**, *102*, 356.
(19) Kawaguchi, M.; Sano, M.; Chen, Y.-L.; Zografi, G.; Yu, H. *Macromolecules* **1986**, *19*, 2606.
(20) Kuzmenka, D. J.; Granick, S. *Polym. Commun.* **1988**, *29*, 64.
(21) Ries, H. E.; Walker, D. C. *J. Colloid Sci.* **1961**, *16*, 361.
(22) Gabrielli, G.; Guarini, G. G. T. *J. Colloid Interface Sci.* **1978**, *64*, 185.
(23) Azzam, R. M. A.; Bashara, N. M. *Ellipsometry and Polarized Light*; North Holland: New York, 1977.
(24) Huglin, M. B., Ed. In *Light Scattering From Polymer Solutions*; Academic: New York, 1972; p 35.
(25) *Polymer Handbook*; Brandrup, J., Immergut, E. H., Eds.; Wiley: New York, 1975.
(26) Strachan, C. S. *Proc. Cambridge Philos. Soc.* **1933**, *29*, 116.
(27) Hall, A. C. *J. Phys. Chem.* **1966**, *70*, 1702.
(28) Sauer, B. B.; Yu, H.; Kim, M. W. *Langmuir*, in press.
(29) *Handbook of Water-Soluble Gums and Resins*; Davidson, R. L., Ed.; McGraw-Hill: New York, 1980.
(30) Rastogi, A. K.; St. Pierre, L. E. *J. Colloid Interface Sci.* **1971**, *35*, 16.

Chain Dimensions in Dilute Polymer Solutions: A Light-Scattering and Viscometric Study of Multiarmed Polyisoprene Stars in Good and Θ Solvents

Barry J. Bauer,[1a] Lewis J. Fetters,*[1b] William W. Graessley,[1c] Nikos Hadjichristidis,[1d] and Günther F. Quack[1e]

Institute of Polymer Science, University of Akron, Akron, Ohio 44325, and Corporate Research Laboratories, Exxon Research and Engineering Company, Annandale, New Jersey 08801. *Received August 31, 1988; Revised Manuscript Received November 23, 1988*

ABSTRACT: The dilute solution properties of long-arm polyisoprene stars with branch point functionality f ranging from 3 to 56 have been investigated both in good solvents (cyclohexane and toluene) and under Θ conditions (1,4-dioxane). The intrinsic viscosity $[\eta]$, Huggins coefficient k_H, second virial coefficient A_2, diffusion coefficient D_0, and radius of gyration R_G were measured and compared in terms of the equivalent radii. A smooth evolution of properties with increasing f was found, leading eventually to what we have termed a fuzzy-sphere behavior at high f. Thus, equilibrium properties such as A_2 and R_G move into a spherelike relationship to one another at large f. The dynamical properties, $[\eta]$ and D_0, do likewise, and k_H approaches the hard-sphere value. However, the radii deduced from dynamical properties are consistently smaller than those from equilibrium properties, suggesting the analogy between polymeric stars of larger functionality and spheres with a hydrodynamically penetrable surface layer. The dependence of size on functionality is different in good and Θ solvents, but the same fuzzy-sphere relationship emerges when f is large. The literature data for polystyrene stars follow the same pattern, being for the most part in quantitative accord with the polyisoprene data. Some unresolved descrepancies in this simple interpretation are pointed out. Good agreement was found between these results and theoretical predictions based on scaling, Monte Carlo calculations, and simulation. Analytical expressions were less satisfactory, especially at high functionality.

Introduction

A study of the dilute solution properties of linear polyisoprene in the thermodynamically good solvent cyclohexane was presented recently.[2] Dilute solution viscometry and light scattering were used to obtain the radius of gyration R_G, the thermodynamic radius R_T, the viscometric radius R_V, and the hydrodynamic radius R_H. The molecular weight dependence of these various measures of coil dimensions was determined. The results were compared with theory and with data for other polymer species. In

0024-9297/89/2222-2337$01.50/0